Title
Impact of autocorrelation on functional connectivity

Journal
NeuroImage, 102(0 2)

ISSN
1053-8119

Authors
Arbabshirani, Mohammad R
Damaraju, Eswar
Phlypo, Ronald
et al.

Publication Date
2014-11-01

DOI
10.1016/j.neuroimage.2014.07.045

Peer reviewed

Published in final edited form as:
Neuroimage. 2014 November 15; 102(0 2): 294–308. doi:10.1016/j.neuroimage.2014.07.045.

Impact of Autocorrelation on Functional Connectivity

Mohammad R. Arbabshirani[a,b,1], **Eswar Damaraju**[a], **Ronald Phlypo**[c], **Sergey Plis**[a], **Elena Allen**[a,d,e], **Sai Ma**[c], **Daniel Mathalon**[f,g], **Adrian Preda**[h], **Jatin G. Vaidya**[i], **Tülay Adali**[c], and **Vince D. Calhoun**[a,b]

[a]The Mind Research Network, Albuquerque, NM, USA

[b]Department of ECE, University of New Mexico, Albuquerque, NM, USA

[c]Department of CSEE, University of Maryland, Baltimore County, MD, USA

[d]K. G. Jebsen Cener for Research on Neuropsychiatric Disorders, University of Bergen, Norway

[e]Department of Biological and Medical Psychology, University of Bergen, Norway

[f]Department of Psychiatry, University of California, San Francisco, CA, USA

[g]San Francisco VA Medical Center, San Francisco, CA, USA

[h]Department of Psychiatry and Human Behavior, University of California, Irvine, CA, USA

[i]Department of Psychiatry, University of Iowa, IA, USA

Abstract

Although the impact of serial correlation (autocorrelation) in residuals of general linear models for fMRI time-series has been studied extensively, the effect of autocorrelation on functional connectivity studies has been largely neglected until recently. Some recent studies based on results from economics have questioned the conventional estimation of functional connectivity and argue that not correcting for autocorrelation in fMRI time-series results in “spurious” correlation coefficients. In this paper, first we assess the effect of autocorrelation on Pearson correlation coefficient through theoretical approximation and simulation. Then we present this effect on real fMRI data. To our knowledge this is the first work comprehensively investigating the effect of autocorrelation on functional connectivity estimates. Our results show that although FC values are altered, even following correction for autocorrelation, results of hypothesis testing on FC values remain very similar to those before correction. In real data we show this is true for main effects and also for group difference testing between healthy controls and schizophrenia patients. We further discuss model order selection in the context of autoregressive processes, effects of frequency filtering and propose a preprocessing pipeline for connectivity studies.

[1]Corresponding author. The Mind Research Network, 1101 Yale Blvd NE, Albuquerque, NM 87106, USA. marbabshirani@mrn.org, Phone: +1 505 272 5028, Fax: +1 505 272 8002.

Keywords

Autocorrelation; Functional Connectivity; Independent Component Analysis; Autoregressive Process; Resting-state fMRI

Introduction

Functional connectivity (FC) is defined as correlation (Friston, 2002) or any other measure of statistical dependency among time series of spatially remote brain voxels/regions. FC analysis describes interactions among brain regions during tasks as well as during resting state scans. In recent years, there has been a debate in the neuroimaging community regarding the possible impact of intrinsic autocorrelation in fMRI time-courses on functional connectivity analysis outcome. Some researchers have even questioned the validity of previous connectivity studies by arguing that not correcting for autocorrelation in fMRI time-series may result in spurious high correlation values (Christova et al., 2011; Georgopoulos and Mahan, 2013). These subject-level studies have confirmed that fMRI time-series are autocorrelated through the use of the Durbin-Watson statistic and have suggested to reduce the autocorrelation by using an autoregressive integrated moving average (ARIMA) model which is called prewhitening (Granger and Morris, 1976; Haugh, 1976).

Autocorrelation in fMRI data is assumed to originate from colored physical and physiological noise (Aguirre et al., 1997; Bullmore et al., 2001; Friston et al., 2000; Lenoski et al., 2008; Lund et al., 2006; Purdon and Weisskoff, 1998; Rajapakse et al., 1998; Zarahn et al., 1997). Several methods have been proposed to deal with autocorrelation in the general linear modeling framework (Friston et al., 2000; Gautama and Van Hulle, 2004; Lund et al., 2006; Woolrich et al., 2001). While some studies have suggested that intrinsic fMRI time-series autocorrelation is negligible compared to smoothing induced autocorrelation (Friston et al., 1995), others found it to be a significant confound (Christova et al., 2011; Lenoski et al., 2008; Zarahn et al., 1997).

It should be noted that most of the recent discussions (Christova et al., 2011; Georgopoulos and Mahan, 2013) are based on previous works in economics and econometrics most notably those initiated by Granger. In his seminal paper, “Spurious regression in economics”, published in 1974, he strongly warned economists regarding the side-effects of ignoring autocorrelated residuals in a regression model (Granger and Newbold, 1974). While these conclusions are fully valid when dealing with just two autocorrelated time-series, to the best of our knowledge, no one has investigated the impact of autocorrelation on functional connectivity based on a careful consideration of the specific differences that reign between the two fields.

In neuroimaging, inference is largely related to hypothesis testing and not necessarily focused on the point estimation of the actual correlation value. Most connectivity analyses are performed at the group level. Answers to questions like “Is the connectivity between two brain regions/networks significant?” or “Is there any significant difference in connectivity between two groups/tasks?” are typically of greater interest than estimating the correlation

coefficients themselves. While most of economics discussion on this issue consider point estimation, it is not clear to what extent autocorrelation affects group level statistics in functional connectivity studies. Another surprising fact is the lack of explicit calculation of the correlation coefficient of two autocorrelated time-series in the literature, at least to the best of our knowledge. The goal of this study is to investigate the impact of autocorrelation on functional connectivity, defined in this study as the Pearson correlation coefficient between time-series of voxels, regions or networks. To better understand the impact of autocorrelation on Pearson correlation coefficient, first, we theoretically derive an approximation of the bias and variance of correlation coefficient estimator in the presence of autocorrelation in a very simple case with the intent to better understand the process (this is distinct from fMRI time-series simulation, which is outside of the scope of this manuscript). These theoretical results don't necessarily generalize to more complicated models due to the simplifying assumptions of this study. This is followed by simulations in order to validate the theoretical results. Finally, the impact of autocorrelation on real resting-state fMRI time-series is assessed. We also discuss proper preprocessing for connectivity analysis based on these observations. We focus on the resting-state FC given the growing interest in this condition and to avoid the confound that autocorrelation in task-based fMRI heavily depends on the task design.

Theoretical Background

Pearson Correlation Coefficient of Two Autocorrelated Time-Series

The most well-known method to model autocorrelation in a time-series is the Box-Jenkins methodology (Box and Jenkins, 1970). In this method, the time-series are observed as outputs of autoregressive integrated moving average (ARIMA) processes. Since calculating the correlation coefficient between two time-series can quickly become highly involved in high ARIMA model orders, we try to assess the impact of autocorrelation in a simple case. Let *w* and *z* denote two white bivariate normally distributed time-series. The Pearson correlation coefficient is defined as the covariance between two random processes divided by the product of their standard deviations:

$$\rho_{w,z}=\frac{cov(w,z)}{\sqrt{var(w)var(z)}} \quad (1)$$

$\rho_{w,z}$ measures the normalized linear dependency between *w* and *z*. In practice, the correlation coefficient is estimated from a limited sample from random variables *w* and *z*:

$$r_{w,z}=\frac{\sum_{i=1}^{N}(w_i-\overline{w})(z_i-\overline{z})}{\sqrt{\sum_{i=1}^{N}(w_i-\overline{w})^2}\sqrt{\sum_{i=1}^{N}(z_i-\overline{z})^2}} \quad (2)$$

where *N* is the number of samples and $\bar{w}$ and $\bar{z}$ are the empirical mean values of *w* and *z*. Distribution of Pearson correlation coefficient is provided in the supplementary material. The first two moments of $r_{w,z}$ are:

$$E[r_{w,z}] \cong \rho_{w,z} - \frac{\rho_{w,z}(1-\rho_{w,z}^2)}{2N} \quad (3)$$

$$var(r_{w,z}) \cong \frac{(1-\rho_{w,z}^2)^2}{N}\left(1+\frac{11\rho_{w,z}^2}{2N}\right) \quad (4)$$

It can be read from Eq. (3) that $r_{w,z}$ is a biased estimator unless $\rho_{w,z}$ is zero.

We assume that *w* and *z* are latent random variables only observable through their respective autocorrelated time-series x and y. We are interested in the true correlation coefficient between *x* and *y* without the induced effect of autocorrelation. In other words, our interest is the genuine Pearson correlation coefficient between *x* and *y* which is the correlation between *w* and z, $\rho_{w,z}$. However, we observe only x and y, autocorrelated versions of w and z, respectively, and their correlation coefficient, $\rho_{x,y}$. We assume that the time-series are in stationary state. Also, we assume that time-series are de-meaned and de-trended without loss of generality, since the time-series can always be de-meaned and de-trended empirically. Moreover, this is almost always part of the preprocessing of functional connectivity analysis. We denote the sample correlation coefficient between *w* and *z* and between *x* and *y* with $r_{w,z}$ and $r_{x,y}$ respectively. Sample variances of *w*, *z*, *x* and *y* are denoted by s_w^2, s_z^2, s_x^2 and s_y^2, respectively. The variables $s_{w,z}$ and $s_{x,y}$ denote sample covariance between (*w* and *z*) and (*x* and *y*), respectively. We consider simple case of autoregressive process of model order one as an example to understand the impact of autocorrelation of correlation coefficient. Note that, we do not intend to simulate fMRI time-series here because of its complex structure of signal and noise. In order to study the effect of autocorrelation on correlation coefficient, we derive an approximate bias and variance of correlation coefficient estimator, $r_{x,y}$ with respect to autocorrelation coefficients and true empirical correlation coefficient, $r_{w,z}$.

Autoregressive process of order one: AR(1)—An AR(1) process can be written in its recursive form as:

$$x_t = \alpha x_{t-1} + w_t \quad (5)$$

$$y_t = \beta y_{t-1} + z_t \quad (6)$$

where the subscript *t* denotes the time index in the time-series and α and β are AR(1) coefficients of absolute value less than 1. This condition is necessary for *x* and *y* to be stationary. First, we calculate the variance of *x* and *y*. Since *x* and *y* are demeaned, the first moments of both series are zero. Also, without loss of generality—and for sake of simplicity—we may assume that initial point in both series is zero. The expected value of the sample variance can be derived and expressed as follows:

$$E[s_x^2]=E[\sum_{i=1}^{N}\frac{x_i^2}{N-1}]=\frac{1}{N-1}\left[\frac{N}{1-\alpha^2}-\frac{1-\alpha^{2N}}{(1-\alpha^2)^2}\right]E[s_w^2] \quad (7)$$

$$E[s_y^2]=E[\sum_{i=1}^{N}\frac{y_i^2}{N-1}]=\frac{1}{N-1}\left[\frac{N}{1-\beta^2}-\frac{1-\beta^{2N}}{(1-\beta^2)^2}\right]E[s_z^2] \quad (8)$$

The expected value of the sample covariance between *x* and *y* can be calculated in the same fashion:

$$E[s_{x,y}]=E[\sum_{i=1}^{N}\frac{x_i y_i}{N-1}]=\frac{1}{N-1}\left[\frac{N}{1-\alpha\beta}-\frac{1-(\alpha\beta)^{2N}}{(1-\alpha\beta)^2}\right]E[s_{w,z}] \quad (9)$$

In order to find the expected value of $r_{x,y}$, we need to calculate:

$$E[r_{x,y}]=E[\frac{s_{x,y}}{\sqrt{s_x^2 s_y^2}}] \quad (10)$$

which is theoretically complicated. In order to be able to simplify (10), we propose first-order multivariate Taylor series expansion approximation of the mean (see Supplementary Material for more details) which is commonly used in many scientific and engineering applications (Ang and Tang, 1975; Hahn and Shapiro, 1967):

$$E[r_{x,y}] \cong \frac{E[s_{x,y}]}{\sqrt{E[s_x^2]E[s_y^2]}} \quad (11)$$

Eq. (11) enables us to simplify Eq. (10) by replacing corresponding terms in Eq. (10) with Eq. (7-9). So, the approximate expected value of sample correlation between *x* and *y* can be calculated as follows:

$$E[r_{x,y}] \cong \frac{\frac{1}{N-1}\left[\frac{N}{1-\alpha\beta}-\frac{1-(\alpha\beta)^{2N}}{(1-\alpha\beta)^2}\right]E[s_{w,z}]}{\sqrt{(\frac{1}{N-1}\left[\frac{N}{1-\alpha^2}-\frac{1-\alpha^{2N}}{(1-\alpha^2)^2}\right]E[s_w^2])(\frac{1}{N-1}\left[\frac{N}{1-\beta^2}-\frac{1-\beta^{2N}}{(1-\beta^2)^2}\right]E[s_z^2])}} \quad (12)$$

If we use the proposed approximation in Eq. (11) in reverse direction the above equation can be simplified as:

$$E[r_{x,y}] \cong \frac{\left[\frac{N}{1-\alpha\beta}-\frac{1-(\alpha\beta)^{2N}}{(1-\alpha\beta)^2}\right]}{\sqrt{\left[\frac{N}{1-\alpha^2}-\frac{1-\alpha^{2N}}{(1-\alpha^2)^2}\right]\left[\frac{N}{1-\beta^2}-\frac{1-\beta^{2N}}{(1-\beta^2)^2}\right]}}E[r_{w,z}] \quad (13)$$

The first result is that the expected value of correlation coefficient between *x* and *y* is approximately a linear function of the expected value of correlation coefficient between *w* and *z*. Asymptotically (as $N \to \infty$), equation (13) reduces to:

$$E[r_{x,y}] \cong \frac{\sqrt{(1-\alpha^2)(1-\beta^2)}}{(1-\alpha\beta)} E[r_{w,z}] \quad (14)$$

Equation (14) tells us that the asymptotic expected value of approximate correlation coefficient between *x* and *y* is always smaller than or equal to the expected value of the correlation coefficient between *w* and *y* since the numerator is always equal or smaller than the denominator. Expected values of $r_{x,y}$ and $r_{w,z}$ are approximately equal only if $\alpha = \beta$. As the distance between α and β increases, expected value of $r_{x,y}$ shrinks towards zero. The variance of the sample correlation coefficient estimator when the time-series follow an AR(1) model and with true correlation, $\rho_{w,z}$ equal to zero was approximated about 80 years ago (Bartlett, 1935):

$$var(r_{x,y}) \cong \frac{1}{N} \frac{1+\alpha\beta}{1-\alpha\beta}. \quad (15)$$

In the above equation $1/N$ is the variance of the estimator when the true correlation between *w* and *z* is zero. We propose to generalize (15) to the case of non-zero $\rho_{w,z}$ by replacing $1/N$ in (15) with the first term in (4):

$$var(r_{x,y}) \cong \frac{(1-\rho_{w,z}^2)^2}{N} \frac{1+\alpha\beta}{1-\alpha\beta} \quad (16)$$

The variance of the estimator, $r_{x,y}$, approximately decreases as the absolute value of the true correlation, $\rho_{w,z}$ increases. The most important observation is that this variance increases as the product of autoregressive parameters, $\alpha\beta$, increases. In other words, autocorrelation reduces the effective degrees of freedom for variance of the sample Pearson correlation coefficient which is a well-known phenomenon (Davey et al., 2013; Friston et al., 1994; Kruggel et al., 2002).

Autoregressive Processes in the Frequency Domain—It is useful to look at the autoregressive process in the frequency domain. The autoregressive process can be modeled as a linear time-invariant (LTI) system with input w_t, impulse response of h_t and output of x_t. Note that all signals are defined over discrete time. It is easy to show that for positive and negative values of α, $H(e^{jw})$ is a lowpass and highpass filter respectively (Supplementary Materials). As $|\alpha|$ (AR1 coefficient) increases the filter becomes sharper. We expect fMRI time-series to exhibit positive autocorrelation which corresponds to a low-pass filter. The purpose of autocorrelation correction is to cancel out the effect of this low-pass filter by applying a filter with inverse frequency response.

Methods

Simulated Data

The statistical software R was used to generate simulated datasets under different scenarios. First, two spectrally white time-series (w and z) were generated from a bivariate normal distribution with different lengths, $N \in \{64, 256, 1024\}$ and correlation, ρ from -0.9 to +0.9 in 0.1 increments. Then, x and y were generated from w and z using Eq. (5) and Eq. (6) with different a and β values. Each simulation scenario was repeated 10,000 times. The mean and standard deviation of $r_{w,z}$ and $r_{x,y}$ were calculated from the 10,000 collected samples. These values were compared to those derived from theoretical estimates as detailed in the previous section.

Real fMRI Data

Participants—For this study we used data from "Functional Imaging Biomedical Informatics Research Network" known as FBIRN. 195 patients with schizophrenia and 175 healthy volunteers were recruited that were matched for age, gender, handedness, and race distributions. All patients included in the study had been diagnosed with schizophrenia based on the Structured Clinical Interview for DSM-IV-TR Axis I Disorders (SCID-I/P) (First, Spitzer, Gibbon, & Williams, 2002a). All patients were clinically stable on antipsychotic medication for at least two months prior to scanning. Additionally, patients with extra pyramidal symptoms and healthy volunteers with a current or past history of major neurological or psychiatric illness (SCIS-I/NP)(First, Spitzer, Gibbon, & Williams, 2002b) or with a first-degree relative with Axis-I psychotic disorder diagnosis were also excluded. Detailed information about participants is provided in the Supplementary Material.

Imaging Parameters—Imaging data for six of the seven sites was collected on a 3T Siemens Tim® Trio System and on a 3T General Electric Discovery MR750 scanner at one site. Resting state fMRI scans were acquired using a standard gradient-echo echo planar imaging paradigm: FOV of 220×220 mm (64×64 matrix), TR = 2 sec, TE = 30 ms, FA = 77^0, 162 volumes, 32 sequential ascending axial slices of 4 mm thickness and 1 mm skip. Subjects had their eyes closed during the resting state scan.

Data preprocessing and quality control—First we computed signal-fluctuation-to-noise (SFNR) (Friedman et al., 2006) for all 370 subjects' EPI data sets as implemented in the *dataQuality* matlab package (http://cbi.nyu.edu/software/dataQuality.php). We performed rigid body motion correction using the INRIAlign (Freire and Mangin, 2001) toolbox in SPM to correct for subject head motion. All subjects that had SFNR < 150 and a maximum root mean squared translation > 4 mm were excluded from further analysis. This excluded a total of 56 subjects, resulting in 314 subjects (163 HC and 151 SZ) for subsequent analysis. For the retained subjects, we performed slice-timing correction to account for timing differences in slice acquisition. Then the fMRI data were despiked using AFNI's 3dDespike algorithm to mitigate the impact of outliers. The fMRI data were subsequently warped to a Montreal Neurological Institute (MNI) template and resampled to 3 mm^3 isotropic voxels. Instead of Gaussian smoothing, we smoothed the data to 6 mm full

width at half maximum (FWHM) using AFNI's BlurToFWHM algorithm which performs smoothing by a conservative finite difference approximation to the diffusion equation. Detailed information regarding data preprocessing and quality control is provided in the Supplementary Material.

Group Independent Component Analysis—All of the preprocessed functional data from both control and patient groups were analyzed using spatial group independent component analysis (GICA) framework as implemented in the GIFT software (Calhoun and Adali, 2012; Calhoun et al., 2001; Erhardt et al., 2011). Spatial ICA decomposes the subject data into linear mixtures of spatially independent components that exhibit a unique time course profile. A subject-specific data reduction step was first used to reduce 162 time point data into 100 orthogonal directions of maximal variability using principal component analysis. Then subject reduced data were concatenated across time and a group data PCA step reduced this matrix further into 100 components along directions of maximal group variability. One hundred independent components were obtained from the group PCA reduced matrix using the *infomax* algorithm (Bell and Sejnowski, 1995). To ensure stability of estimation, we repeated the ICA algorithm 20 times and using ICASSO[2] aggregate spatial maps were estimated as the modes of component clusters. Subject specific spatial maps (SMs) and time courses (TCs) were obtained using the spatio-temporal regression back reconstruction approach (Calhoun et al., 2001; Erhardt et al., 2011) implemented in GIFT software.

Post ICA processing—Subject specific SMs and TCs underwent post processing as described in our earlier work (Allen et al., 2012). Briefly, we obtained one sample *t*-test maps for each SM across all subjects and thresholded these maps to obtain regions of peak activation clusters for that component; we also computed mean power spectra of the corresponding TCs. We identified a set of components as intrinsic connectivity networks (ICNs) if their peak activation clusters fell on gray matter and showed less overlap with known vascular, susceptibility, ventricular, and edge regions corresponding to head motion. We also ensured that the mean power spectra of the selected ICN time courses showed higher low frequency spectral power. This selection procedure resulted in 47 ICNs out of the 100 independent components obtained. The cluster stability/quality (I_q) index for these ICNs over 20 ICASSO runs was very high ($I_q > 0.9$) for all of the components, except an ICN that resembles language network ($I_q = 0.74$).

The subject specific TCs corresponding to the ICNs selected were detrended (with polynomial of order two), orthogonalized with respect to estimated subject motion parameters, and then despiked. The despiking procedure involved detecting spikes as determined by AFNI's 3dDespike algorithm and replacing spikes by values obtained from third order spline fit to neighboring clean portions of the data. The despiking process reduces the impact/bias of outliers on subsequent functional network connectivity (FNC) measures (Allen et al., 2012).

[2] http://www.cis.hut.fi/projects/ica/icasso

It is important to note that raw fMRI time-series are not stationary with respect to the mean due to many factors such as the scanner drift. This undesired property violates an important assumption in many statistical procedures. The common practice in analyzing fMRI time-series is to detrend them (e.g. by polynomial of order 2). This preprocessing step makes the stationary assumption much more realistic.

Functional Network Connectivity—There is growing interest in studying functional connectivity among brain functional networks. This type of connectivity, which can be considered as a higher level of FC, is termed functional network connectivity (FNC) (Jafri et al., 2008) and measures the statistical dependencies among brain functional networks. Each functional network may consist of multiple remote brain regions. Spatial components resulting from sICA are maximally spatially independent but their corresponding time-courses can show a considerable amount of temporal dependency. This property of sICA makes it an excellent choice for studying FNC, which can be studied by analyzing these weaker dependencies among sICA time courses. Our real fMRI results focuses on FNC but the results are also applicable to FC since both forms of connectivity use correlation coefficient among time-series (FNC can be thought of as FC using a weighted seed map (Joel et al., 2011)). We use the term “uncorrected FC/FNC” to describe correlations between the original time series, whereas “correct FC/FNC” describes correlations between the autocorrelation corrected time-series hereafter.

Autocorrelation Correction

AR models with orders ranging from 1 to 15 were fit to each ICA time-series for each subject. The best model order was selected based on the Akaike information criterion (AIC) (Akaike, 1974). The residuals of the best model were used as the corrected, white time-series. The Durbin-Watson (DW) statistic is a common statistic to measure autocorrelation in a time-series (Durbin and Watson, 1950, 1951). A DW statistic of 2 signifies no autocorrelation and DW values less or greater than 2 signify positive and negative autocorrelation structure, respectively. The DW statistics for a time-series (w_t) with N time points can be calculated as follows:

$$d=\frac{\sum_{t=2}^{N}(w_t - w_{t-1})^2}{\sum_{t=1}^{N} w_t^2} \quad (17)$$

Results

Simulated Data

The theoretical results in the previous sections established the properties of the sample correlation coefficient between two autocorrelated time-series ($r_{x,y}$). To verify the validity of the theoretical results, time-series w, z, x and y were simulated with different α, β, N and $\rho_{w,z}$ values (see Materials and Methods section for more details). The empirical bias of $r_{w,z}$ and $r_{x,y}$ was computed by subtracting $\rho_{w,z}$ from mean of $r_{w,z}$ and $r_{x,y}$ averaged over 10,000 runs respectively. The empirical standard deviation of observed $r_{w,z}$ and $r_{x,y}$ averaged over 10,000 runs is also reported. In Figure 1A summary of the simulation and theoretical results

for $\rho_{w,z} = 0.5$ is depicted. The results for other correlation values are omitted from the main text since results followed Eq. (13) and Eq. (16), similar to the case of $\rho_{w,z} = +0.5$, though results for $\rho_{w,z} = +0.2$ and $\rho_{w,z} = +0.8$ are provided in the supplementary material. The bias for negative values of $\rho_{w,z}$ was of the same size as for the positive values but in the opposite direction (bias was positive); variance for negative and positive $\rho_{w,z}$ were the same. It is evident from Figure 1A that our theoretical approximations follow the empirical results closely. In only extreme autocorrelation coefficient values (e.g. $\alpha = \beta = 0.9$) our theoretical approximation overestimate the empirical variance.

To better portray the effect of autocorrelation on correlation coefficients in the simulated data, Figure 1B displays histograms of $r_{w,z}$ and $r_{x,y}$ as well as scatter plot of $r_{x,y}$ against $r_{w,z}$ for three simulation scenarios, all with a sample size of 256. These 3 cases were selected based on the plausible AR(1) coefficient for real fMRI data. Note that Figure 1A shows average of 10,000 runs for each scenario while Figure 1B shows the histogram and scatterplots of all 10,000 values for the selected cases.

Real fMRI Data

After standard preprocessing, the functional imaging data from all subjects was decomposed into a set of 100 statistically independent spatial regions with common time course profile using group independent component analysis using GIFT toolbox (http://mialab.mrn.org/software/gift). Subject-specific spatial maps and time courses were obtained using spatio-temporal regression (Erhardt et al., 2011). Of these 100 components, 47 components were identified as resting-state networks using the procedures described in our earlier work (Allen et al., 2012; Allen et al., 2011). For each subject, we computed the functional network connectivity, referred to as FNC, by computing pairwise Pearson correlation using the whole processed ICA time-courses resulting in 1081 connectivity values. ICA spatial maps were broadly categorized based on anatomical proximity and prior knowledge of their function into the following sub-categories: subcortical (SC), auditory (AUD), visual (VIS), somatomotor (SM), a heterogeneous set of regions involved in various attentional and cognitive control processes (CC), default-mode (DMN), and cerebellar (CB) networks. These resting-state networks are illustrated in Figure 2.

To assess the impact of autocorrelation on FC, ICA-time courses were corrected using autoregressive model. Best AR model order was selected based on AIC. The Durbin-Watson statistic was used to measure autocorrelation in the time-series before and after autocorrelation correction. Histograms of the DW statistics of ICA time-series for both healthy and patient groups before and after autocorrelation correction are plotted in Figure 3.

We also performed a one-sample t-test on Fisher-Z transformed FNC values. The mean and standard deviation of FNC values along with corresponding p-values before and after autocorrelation correction for both healthy controls and schizophrenia patients are reported in Figure 4A,B and 5A,B respectively. It is evident that both mean and standard deviation are inflated before autocorrelation correction. The bias in the mean and standard deviation of FNC values cancel each other significantly in the t-tests as illustrated in Figure 4C and 5C making the hypothesis testing results very similar before and after correction.

One of the common purposes of connectivity analysis is to compare groups (e.g. healthy controls and patients). To investigate the effect of autocorrelation on such problems, FNC was compared between healthy controls and schizophrenia patients using two-sample t-test before and after autocorrelation correction. The resulting p-values along with the difference in FNC before and after autocorrelation correction are illustrated in Figure 6.

To better observe the relationship between FNC values before and after autocorrelation correction, histogram of FNC values (all pairs for all subjects pooled) before and after autocorrelation correction are plotted in Figure 7(A). Scatter plots of uncorrected FNC values (pooled) against corrected FNC values are illustrated in Figure 7(B). We also plotted $-\log(p\_value) \times sign(T\_Statistics)$ (Figure 4C, 5C) before and after correction for both groups in Figure 7(C) which shows a strong linear relationship.

We also repeated the autocorrelation correction with just an AR(1) model to determine the range of AR(1) coefficients for real fMRI data and compare it to the theoretical and simulation results. The model worked reasonably well based on DW statistics. The histogram of AR(1) coefficients for healthy controls and schizophrenia patients are illustrated in Figure 8:

Discussion

In this work, we comprehensively investigated the impact of autocorrelation on functional connectivity with theory, simulations and real fMRI data. We derived the approximate bias and variance of Pearson correlation coefficient for two autocorrelated time-series (x,y) with AR(1) structure as an estimator of the true correlation coefficient between white time-series component of the AR(1) models (w,z). Based on Eq. (13), approximately the expected value between two autocorrelated time-series is equal or less than the expected value between the white latent time-series in the AR(1) model. If the AR(1) coefficients for both time-series are equal, the estimation is unbiased. The estimation becomes biased as the distance between AR coefficients of the two time-series increases. Based on Eq. (16), the variance of this estimator increases as the product of the AR(1) coefficient of the two time-series increases.

The autoregressive process has been investigated heavily in signal processing domain from frequency point of view. The AR(1) process has been modeled as a linear time-invariant system with a white time-series input and autocorrelated time-series as the output (Figure S1). It was seen that feeding an AR(1) model (positive coefficient) with a white signal results in a lowpassed output signal (Figure S2). The process of autocorrelation correction (whitening) can be viewed as applying frequency response of the inverse system to the observed signal to even out the frequency spectrum.

Figure 1A shows how bias and variance of estimation of $\rho_{w,z}$ changes based on theoretical and empirical results of $r_{w,y}$ and $r_{w,z}$ with respect to AR(1) coefficients. It is evident that empirical results agree with and validate the theoretical results at least in the context of this study. It is also clear that the bias in estimation of $r_{w,z}$ based on $r_{x,y}$ is a function of distance between AR(1) coefficients of x and y while the variance is a function of the product of AR(1) coefficients. To better investigate the effect of autocorrelation on Pearson correlation

coefficient, histogram of $r_{w,z}$ and $r_{x,y}$ as well as scatter plot of $r_{x,y}$ against $r_{w,z}$ for 3 different AR(1) coefficient pairs were illustrated in Figure 1B. The bias and variance effect of autocorrelation on estimating $r_{w,z}$ based on $r_{x,y}$ is obvious in these 3 simulations.

For real fMRI data, the FC values before and after autocorrelation correction show noticeable difference in both healthy controls and patients (Figure 4A, 5A). We see the same pattern in standard deviation (Figure 4B, 5B). The direction of change for both mean and standard deviation is the same. As a result, the p-values resulting from one-sample t-tests on each FC value across subjects are very similar before and after autocorrelation correction (Figure 4C, 5C). In other words, bias in the mean is cancelled out significantly by bias in the standard deviation in the t-tests. The inflation in standard deviation of the correlation values is in line with theoretical results (Eq. 16) and simulation results (Figure 1). This is more clearly depicted in Figure 7C. This suggests that inference related to the significance of FC is not strongly affected by autocorrelation correction. This interesting result argues against the recent debates about spuriousness of functional connectivity based on uncorrected correlation coefficient (Christova et al., 2011; Georgopoulos and Mahan, 2013). While the argument regarding the correlation values themselves remain valid, it appears that hypothesis testing remains relatively unbiased in the presence of autocorrelation. This observation is also present in differences in FC between healthy controls and schizophrenia patients (Figure 6). As illustrated in Figure 7, corrected and uncorrected functional network connectivity values are highly correlated with each other and exhibit a linear relationship. The scatter plots of p-values before and after autocorrelation correction show even stronger linear relationship as illustrated in Figure 7C. The uncorrected FNC values show larger variance compared to the corrected values, as expected from Eq. (16). In order to compare the real fMRI data with the simulation results, we also corrected for autocorrelation using AR(1) model. Based on DW statistics, AR(1) model was able to remove the autocorrelation reasonably well. The histogram of AR(1) model coefficients as illustrated in Figure 8 shows that the fMRI time-series in this study have AR(1) coefficients less than +0.8 and mostly in the range of [+0.1 +0.7]. Thus we don't expect to see the extreme cases in real fMRI that we observed in the simulation results (Figure 1).

It should be noted that in cases where the correlation coefficient itself is of interest, autocorrelation correction is more critical. However, it is always recommended to check for autocorrelation structure in fMRI time-series. Although the statistical analysis in this study was conducted using R software, we provide MATLAB code for autocorrelation correction as it is the main technical computing software used by neuroimaging community[3]. There are several important issues regarding autocorrelation correction that we discuss below.

Autocorrelation correction and Frequency Filtering

Temporal filtering is one the common preprocessing steps in functional connectivity studies. The reason for temporal filtering is that it is believed that signals of interest in connectivity studies reside in a narrow frequency band mainly from 0.01 Hz to 0.08~0.15 Hz (Auer, 2008; Biswal et al., 1995; Cordes et al., 2001; Salvador et al., 2005; Zhong et al., 2009)

[3] http://mialab.mrn.org/software/autox_correction/index.html

while scanner drift and physiological noise are in lower and higher frequency, range respectively (Bianciardi et al., 2009; Lowe et al., 1998; Thomas et al., 2002). Although some functional connectivity studies have shown that temporal filtering does not significantly impact the results in group studies(Arbabshirani et al., 2013a), it is a common practice. It should be noted that modifying frequency spectrum of a signal with filtering changes the autocorrelation profile of the signal. Specifically, frequency filtering of a white signal induces autocorrelation. Thus, if fMRI time-series are corrected for their intrinsic autocorrelation with methods like ARIMA, frequency filtering can introduce a more complicated autocorrelation problem (Davey et al., 2013). This is demonstrated in Figure 9.

In this example, two real fMRI time-series are shown along with their amplitude frequency spectra and autocorrelation functions. Some values of the autocorrelation function are outside the 95% confidence interval indicating significant autocorrelation. Also, the frequency spectra are not flat. After applying AR(4) model to correct both time-series, the frequency spectra are closer to flat and autocorrelation functions is bounded inside the 95% confidence interval. Applying a bandpass frequency filter (0.01-0.10 Hz), reintroduces autocorrelation to an even more severe degree than compared to the intrinsic fMRI autocorrelation. This problem has been studied carefully and a correction on the correlation values between filtered time-series has been proposed based on degrees of freedom correction which is related to filter parameters (Davey et al., 2013). The assumption in this method is that two time-series are white before filtering. A reasonable preprocessing for connectivity studies is to correct for autocorrelation, perform frequency filtering, and then correct the correlation values based on the filter parameters.

Model order for Autocorrelation Correction

One of the main issues in autocorrelation correction is the model order selection problem. As briefly discussed in the introduction, autocorrelation in fMRI time-series originates from physical and physiological noise. One of the main sources of autocorrelation is the hemodynamic response function (Friston et al., 1995; Rajapakse et al., 1998). FMRI time-series can be seen as samples from the hemodynamic response function (HRF) with sampling rate of $1/TR$ where TR is the repetition time of the scanner. Since the HRF is a smooth curve, samples exhibit autocorrelation. A faster TR results in a higher sample rate but come with higher autocorrelation, thus model order should be directly related to TR. Assume that there is a single event fMRI time-series. In this case the resulting time-series is the sampled HRF. We sampled the HRF with different TRs and corrected for autocorrelation by finding the best AR model order based on AIC. Figure 10A show a canonical HRF function. Figure 10B plots TR against the estimated model order. The best AR model order grows exponentially as TR decreases. This example is for a single event while typical task-based fMRI consists of series of events or blocks which can result in different autocorrelation structure. However, Figure 10B gives a rough idea of the model order required to correct for autocorrelation, and shows that autocorrelation correction becomes more crucial as the experimental TR decreases.

Impact of Autocorrelation on FC: Hyperconnectivity, Hypoconnectivity or No Impact?

In regression analysis it has been shown that estimation of model parameters (β) in the presence of serial correlation in the residuals is still unbiased but not efficient (Granger and Morris, 1976; Monti, 2011). It is important not to extend this result to the impact of autocorrelation on functional connectivity. Autocorrelation can bias the estimation of Pearson correlation coefficient based on our theoretical, simulated and real fMRI results. Eq. (13) as demonstrated by our empirical results in Figure 1A, shows that if AR(1) coefficient of the two time-series differ, then the Pearson correlation coefficient is underestimated. If the coefficients are the same, then the estimation is unbiased. These results are plausible since we consider AR(1) as a filter (Figure S1 and S2), then applying the same filter to two white time-series should not change their correlation coefficient but applying different filters can reduce it. However, our real fMRI results in Figures 4 & 5 are consistent with other studies (Christova et al., 2011; Davey et al., 2013), suggest hyperconnectivity for uncorrected time-series, seemingly contradicting our theoretical and simulation results. The approximate theoretical results are just for AR(1) process while the real fMRI data was corrected with AR of order 1 to 15 based on AIC criterion. Also, it is assumed that the two time-series are uniformly correlated with respect to frequency. In other words, correlation is equally present in all frequency bands between w and z. This assumption is not generally true for real fMRI time-series. fMRI time-series consists of a low frequency component that is the major source of correlation which is corrupted with noise that is assumed to be more in higher frequencies (Cordes et al., 2001). Thus, applying a low pass filter can remove the noise (or part of the noise) and enhance the correlation between the two time-series. To better illustrate this, we simulated a simple case where two correlated low frequency time-series (Figure 11A) were generated and then high frequency noise was added (Figure 11B). Finally the noisy signals were passed through an AR(1) process (Figure 11C).

It is evident that autocorrelation (Figure 11C) behaves as a low pass filter as expected (refer to supplementary material for more detailed discussion) and removes part of the high frequency noise and therefore enhanced the correlation compared to the noisy situation (Figure 11B). Note that this increased correlation is very close to the original correlation between the two time-series before adding noise (Figure 11A). So, autocorrelation process is capable of removing noise (depending on the model order, coefficients and frequency spectra of the signals) and increasing correlation. We believe that this is the primary reason for hyperconnectivity in uncorrected functional connectivity studies. Despite the hyperconnectivity, the result of hypothesis tests such as the t-test remain similar for corrected and uncorrected FC values since overestimation of the mean is significantly compensated with the bias in standard error of the mean (Figures 4,5 & 7). This simple example shows that autocorrelation correction may result in unwanted amplification of high frequency bands that is assumed to be dominated by noise in fMRI time-series.

Limitations and Future Studies

The current study compares FC before and after autocorrelation study with a specific choice of analysis pathway. There are several other choices for each analysis step that have not been considered in this study. For example, we removed autocorrelation by using autoregressive model while there are several more advanced methods to model

autocorrelation. For functional connectivity we used group ICA followed by Pearson correlation coefficient among ICA time-courses (FNC). Seed-based analysis is another common method for connectivity studies. Correlation is not the only way of measuring statistical dependency and other methods such as mutual information are common too. We compared FNC before and after autocorrelation correction via t-tests on each FNC value. Although mean and standard error are the main component of many statistical tests such as t-test, we should emphasize that there are several other statistical analysis methods (like multivariate methods) to compare functional connectivity values within a group and between groups. Also, p-values are not the only measures of statistical significance. These choices were guided by our previous functional connectivity studies (Arbabshirani and Calhoun, 2011; Arbabshirani et al., 2013a; Arbabshirani et al., 2013b; Jafri et al., 2008; Meda et al., 2012) and others (Greicius et al., 2003; Wang et al., 2007).

One important subject for future studies is to assess the impact of autocorrelation in task-based studies. Such a study has its own complications since the design paradigm affects the autocorrelation structure in fMRI time-series.

With regard to theoretical results, an interesting topic of future studies may be to investigate the impact of autocorrelation on Pearson correlation in the general case of AR(N) where N is a positive integer. In the case of N>1, autocorrelation affects the time-series as a more flexible frequency filter (compared to AR(1) as discussed in the supplementary material) depending on the AR coefficients which can impact the results differently. Moreover, theoretical results and simulation time-series characteristics could be matched more closely to the settings of real fMRI which is non-trivial due to complex signal and noise structure of fMRI time-series.

Conclusion

In this study, we assessed the effect of autocorrelation on functional connectivity. We started with approximate theoretical results in a simple AR(1) model and provided approximations for bias and variance of estimator of Pearson's correlation coefficient between two autocorrelated time-series. The approximated theoretical results were well validated using simulations. We found that bias of the estimation depends on the difference between AR(1) coefficients of the two time-series while the variance is a function of product of the coefficients. We further investigated the effect of autocorrelation on functional connectivity in real fMRI data in both healthy controls and schizophrenia patients. We found that autocorrelation can slightly alter the Pearson's correlation coefficients, however, the effect of this on the hypothesis tests of group differences based on t-statistics is very mild. It should be noted that the effect of autocorrelation appears to directly depend on the *TR* parameter of the MRI acquisition and the problem becomes more serious for fast acquisitions. Our results do not support the hypothesis that ignoring intrinsic autocorrelation in fMRI time-series results in meaningless spurious connectivity results, unlike some recent studies. While it remains important to assess and correct autocorrelation with appropriate model order to ensure the most accurate results, within the discrete domain of functional connectivity neuroimaging studies it does not appear that autocorrelation has a universally strong and indiscriminate biasing effect.

Supplementary Material

Refer to Web version on PubMed Central for supplementary material.

Acknowledgments

We would like to acknowledge the efforts of all parties responsible for designing and implementing the experiment, collecting the data, and facilitating the brain imaging that made this study possible. Funding was provided by NIH for the FBIRN study (NCRR grant U24-RR021992) and COBRE NIGMS P20GM103472.

References

Aguirre GK, Zarahn E, D'Esposito M. Empirical analyses of BOLD fMRI statistics. II. Spatially smoothed data collected under null-hypothesis and experimental conditions. Neuroimage. 1997; 5:199–212. [PubMed: 9345549]

Akaike H. New Look at Statistical-Model Identification. Ieee Transactions on Automatic Control Ac. 1974; 19:716–723.

Allen EA, Damaraju E, Plis SM, Erhardt EB, Eichele T, Calhoun VD. Tracking Whole-Brain Connectivity Dynamics in the Resting State. Cereb Cortex. 2012

Allen EA, Erhardt EB, Damaraju E, Gruner W, Segall JM, Silva RF, Havlicek M, Rachakonda S, Fries J, Kalyanam R, Michael AM, Caprihan A, Turner JA, Eichele T, Adelsheim S, Bryan AD, Bustillo J, Clark VP, Feldstein Ewing SW, Filbey F, Ford CC, Hutchison K, Jung RE, Kiehl KA, Kodituwakku P, Komesu YM, Mayer AR, Pearlson GD, Phillips JP, Sadek JR, Stevens M, Teuscher U, Thoma RJ, Calhoun VD. A baseline for the multivariate comparison of resting-state networks. Front Syst Neurosci. 2011; 5:2. [PubMed: 21442040]

Ang, AH-S.; Tang, WH. Probability concepts in engineering planning and design. Wiley; New York: 1975.

Arbabshirani MR, Calhoun VD. Functional network connectivity during rest and task: comparison of healthy controls and schizophrenic patients. Conf Proc IEEE Eng Med Biol Soc. 2011; 2011:4418–4421. [PubMed: 22255319]

Arbabshirani MR, Havlicek M, Kiehl KA, Pearlson GD, Calhoun VD. Functional network connectivity during rest and task conditions: a comparative study. Hum Brain Mapp. 2013a; 34:2959–2971. [PubMed: 22736522]

Arbabshirani MR, Kiehl KA, Pearlson GD, Calhoun VD. Classification of schizophrenia patients based on resting-state functional network connectivity. Front Neurosci. 2013b; 7:133. [PubMed: 23966903]

Auer DP. Spontaneous low-frequency blood oxygenation level-dependent fluctuations and functional connectivity analysis of the 'resting' brain. Magn Reson Imaging. 2008; 26:1055–1064. [PubMed: 18657923]

Bartlett MS. Some aspects of the time correlation problem in regard to tests of significance. Journal of the Royal Statistical Society. 1935; 98:536–543.

Bell AJ, Sejnowski TJ. An Information Maximization Approach to Blind Separation and Blind Deconvolution. Neural Computation. 1995; 7:1129–1159. [PubMed: 7584893]

Bianciardi M, Fukunaga M, van Gelderen P, Horovitz SG, de Zwart JA, Shmueli K, Duyn JH. Sources of functional magnetic resonance imaging signal fluctuations in the human brain at rest: a 7 T study. Magnetic resonance imaging. 2009; 27:1019–1029. [PubMed: 19375260]

Biswal B, Yetkin FZ, Haughton VM, Hyde JS. Functional connectivity in the motor cortex of resting human brain using echo-planar MRI. Magnetic resonance in medicine : official journal of the Society of Magnetic Resonance in Medicine / Society of Magnetic Resonance in Medicine. 1995; 34:537–541.

Box, GEP.; Jenkins, GM. Time series analysis; forecasting and control. Holden-Day; San Francisco: 1970.

Bullmore E, Long C, Suckling J, Fadili J, Calvert G, Zelaya F, Carpenter TA, Brammer M. Colored noise and computational inference in neurophysiological (fMRI) time series analysis: resampling methods in time and wavelet domains. Hum Brain Mapp. 2001; 12:61–78. [PubMed: 11169871]

Calhoun VD, Adali T. Multisubject independent component analysis of fMRI: a decade of intrinsic networks, default mode, and neurodiagnostic discovery. IEEE reviews in biomedical engineering. 2012; 5:60–73. [PubMed: 23231989]

Calhoun VD, Adali T, Pearlson GD, Pekar JJ. A method for making group inferences from functional MRI data using independent component analysis. Hum Brain Mapp. 2001; 14:140–151. [PubMed: 11559959]

Christova P, Lewis SM, Jerde TA, Lynch JK, Georgopoulos AP. True associations between resting fMRI time series based on innovations. Journal of neural engineering. 2011; 8:046025. [PubMed: 21712571]

Cordes D, Haughton VM, Arfanakis K, Carew JD, Turski PA, Moritz CH, Quigley MA, Meyerand ME. Frequencies contributing to functional connectivity in the cerebral cortex in “resting-state” data. AJNR American journal of neuroradiology. 2001; 22:1326–1333. [PubMed: 11498421]

Davey CE, Grayden DB, Egan GF, Johnston LA. Filtering induces correlation in fMRI resting state data. Neuroimage. 2013; 64:728–740. [PubMed: 22939874]

Durbin J, Watson GS. Testing for Serial Correlation in Least Squares Regression .1. Biometrika. 1950; 37:409–428. [PubMed: 14801065]

Durbin J, Watson GS. Testing for Serial Correlation in Least Squares Regression .2. Biometrika. 1951; 38:159–178. [PubMed: 14848121]

Erhardt EB, Rachakonda S, Bedrick EJ, Allen EA, Adali T, Calhoun VD. Comparison of multi-subject ICA methods for analysis of fMRI data. Hum Brain Mapp. 2011; 32:2075–2095. [PubMed: 21162045]

Freire L, Mangin JF. Motion correction algorithms may create spurious brain activations in the absence of subject motion. Neuroimage. 2001; 14:709–722. [PubMed: 11506543]

Friedman L, Glover GH, Fbirn C. Reducing interscanner variability of activation in a multicenter fMRI study: controlling for signal-to-fluctuation-noise-ratio (SFNR) differences. Neuroimage. 2006; 33:471–481. [PubMed: 16952468]

Friston K. Beyond phrenology: what can neuroimaging tell us about distributed circuitry? Annual review of neuroscience. 2002; 25:221–250.

Friston K, Jezzard P, Turner R. Analysis of functional MRI time-series. Hum Brain Mapp. 1994; 1:153–171.

Friston KJ, Holmes AP, Poline JB, Grasby PJ, Williams SC, Frackowiak RS, Turner R. Analysis of fMRI time-series revisited. Neuroimage. 1995; 2:45–53. [PubMed: 9343589]

Friston KJ, Josephs O, Zarahn E, Holmes AP, Rouquette S, Poline J. To smooth or not to smooth? Bias and efficiency in fMRI time-series analysis. Neuroimage. 2000; 12:196–208. [PubMed: 10913325]

Gautama T, Van Hulle MM. Optimal spatial regularisation of autocorrelation estimates in fMRI analysis. Neuroimage. 2004; 23:1203–1216. [PubMed: 15528120]

Georgopoulos AP, Mahan MY. Fmri Data Analysis: State of Affairs and Challenges. Quarterly Review of Biology. 2013; 88:121–124.

Granger CWJ, Morris MJ. Time-Series Modeling and Interpretation. Journal of the Royal Statistical Society Series a-Statistics in Society. 1976; 139:246–257.

Granger CWJ, Newbold P. Spurious regressions in econometrics. Journal of Econometrics. 1974; 2:111–120.

Greicius MD, Krasnow B, Reiss AL, Menon V. Functional connectivity in the resting brain: a network analysis of the default mode hypothesis. Proc Natl Acad Sci U S A. 2003; 100:253–258. [PubMed: 12506194]

Hahn, GJ.; Shapiro, SS. Statistical models in engineering. Wiley; New York: 1967.

Haugh LD. Checking Independence of 2 Covariance-Stationary Time-Series - Univariate Residual Cross-Correlation Approach. Journal of the American Statistical Association. 1976; 71:378–385.

Jafri MJ, Pearlson GD, Stevens M, Calhoun VD. A method for functional network connectivity among spatially independent resting-state components in schizophrenia. Neuroimage. 2008; 39:1666–1681. [PubMed: 18082428]

Joel SE, Caffo BS, van Zijl PC, Pekar JJ. On the relationship between seed-based and ICA-based measures of functional connectivity. Magn Reson Med. 2011; 66:644–657. [PubMed: 21394769]

Kruggel F, Pelegrini-Issac M, Benali H. Estimating the effective degrees of freedom in univariate multiple regression analysis. Medical image analysis. 2002; 6:63–75. [PubMed: 11836135]

Lenoski B, Baxter LC, Karam LJ, Maisog J, Debbins J. On the Performance of Autocorrelation Estimation Algorithms for fMRI Analysis. Ieee Journal of Selected Topics in Signal Processing. 2008; 2:828–838.

Lowe MJ, Mock BJ, Sorenson JA. Functional connectivity in single and multislice echoplanar imaging using resting-state fluctuations. NeuroImage. 1998; 7:119–132. [PubMed: 9558644]

Lund TE, Madsen KH, Sidaros K, Luo WL, Nichols TE. Non-white noise in fMRI: does modelling have an impact? Neuroimage. 2006; 29:54–66. [PubMed: 16099175]

Meda SA, Gill A, Stevens MC, Lorenzoni RP, Glahn DC, Calhoun VD, Sweeney JA, Tamminga CA, Keshavan MS, Thaker G, Pearlson GD. Differences in resting-state functional magnetic resonance imaging functional network connectivity between schizophrenia and psychotic bipolar probands and their unaffected first-degree relatives. Biological psychiatry. 2012; 71:881–889. [PubMed: 22401986]

Monti MM. Statistical Analysis of fMRI Time-Series: A Critical Review of the GLM Approach. Front Hum Neurosci. 2011; 5:28. [PubMed: 21442013]

Purdon PL, Weisskoff RM. Effect of temporal autocorrelation due to physiological noise and stimulus paradigm on voxel-level false-positive rates in fMRI. Hum Brain Mapp. 1998; 6:239–249. [PubMed: 9704263]

Rajapakse JC, Kruggel F, Maisog JM, von Cramon DY. Modeling hemodynamic response for analysis of functional MRI time-series. Hum Brain Mapp. 1998; 6:283–300. [PubMed: 9704266]

Salvador R, Suckling J, Coleman MR, Pickard JD, Menon D, Bullmore E. Neurophysiological architecture of functional magnetic resonance images of human brain. Cerebral cortex. 2005; 15:1332–1342. [PubMed: 15635061]

Thomas CG, Harshman RA, Menon RS. Noise reduction in BOLD-based fMRI using component analysis. NeuroImage. 2002; 17:1521–1537. [PubMed: 12414291]

Wang K, Liang M, Wang L, Tian L, Zhang X, Li K, Jiang T. Altered functional connectivity in early Alzheimer's disease: a resting-state fMRI study. Hum Brain Mapp. 2007; 28:967–978. [PubMed: 17133390]

Woolrich MW, Ripley BD, Brady M, Smith SM. Temporal autocorrelation in univariate linear modeling of FMRI data. Neuroimage. 2001; 14:1370–1386. [PubMed: 11707093]

Zarahn E, Aguirre GK, D'Esposito M. Empirical analyses of BOLD fMRI statistics. I. Spatially unsmoothed data collected under null-hypothesis conditions. Neuroimage. 1997; 5:179–197. [PubMed: 9345548]

Zhong Y, Wang H, Lu G, Zhang Z, Jiao Q, Liu Y. Detecting functional connectivity in fMRI using PCA and regression analysis. Brain Topogr. 2009; 22:134–144. [PubMed: 19408112]

Highlights

- The effect of autocorrelation on functional connectivity (FC) has been investigated
- We study autocorrelation in theory, simulations and real fMRI data
- Model order selection and proper preprocessing for FC studies has been discussed

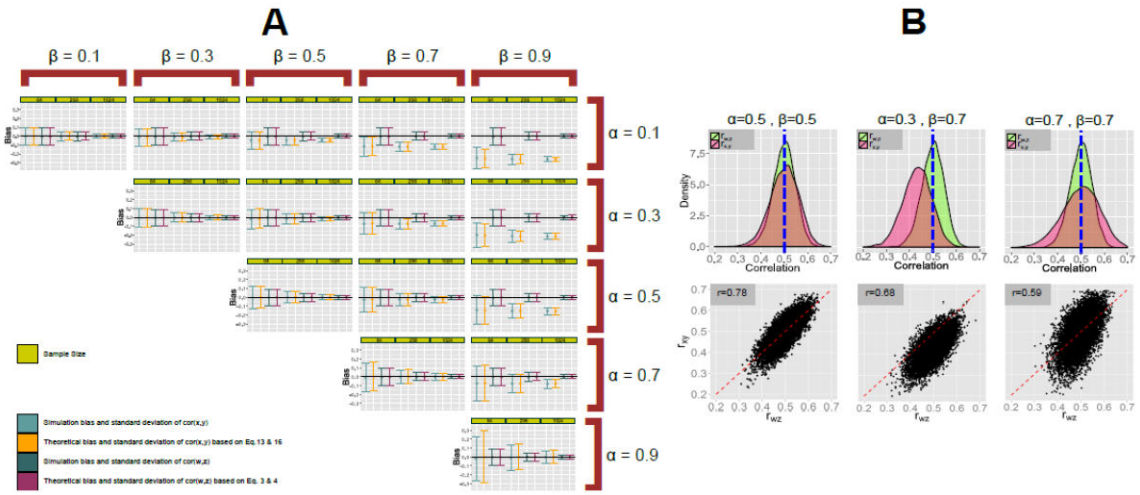

Figure 1.

A) Empirical bias and standard deviation of estimation of true $\rho_{w,z}$ = +0.5 based on $r_{x,y}$ and $r_{w,z}$ for different combinations of AR(1) coefficients (α and β in Eq. (5) & (6)) for time-series x and y and different sample sizes (length of time-series x and y) of (64, 256, 1024) obtained from 10000 simulations. The empirical results are compared with theoretical bias and standard deviation of $r_{w,z}$ and $r_{x,y}$ derived in Eq. (3) & (4) and Eq. (13) & (16) respectively. The whiskers show standard deviation (square root of variance of the estimator). It is evident that theoretical and empirical results agree with each other. For equal coefficients, estimation of $\rho_{w,z}$ based on $r_{x,y}$ is unbiased. For different AR(1) coefficients, estimation is biased. The variance of the estimator increases as the product of AR(1) coefficients of x_t and y_t increases. **B)** Top row: Histogram of corrected and uncorrected empirical Pearson correlation coefficients ($r_{w,z}$ and $r_{x,y}$) obtained from 10000 simulations based on Eq. (5) & (6) with sample size of 256 and true correlation of +0.5 for 3 different combination of α and β (Eq. 5 & 6). Bottom Row: Scatter plot of uncorrected correlation coefficients, $r_{x,y}$, against corrected correlation coefficients $r_{w,z}$. Correlation coefficient between $r_{w,z}$ and $r_{x,y}$ is provided in the bottom row scatter plots (r).

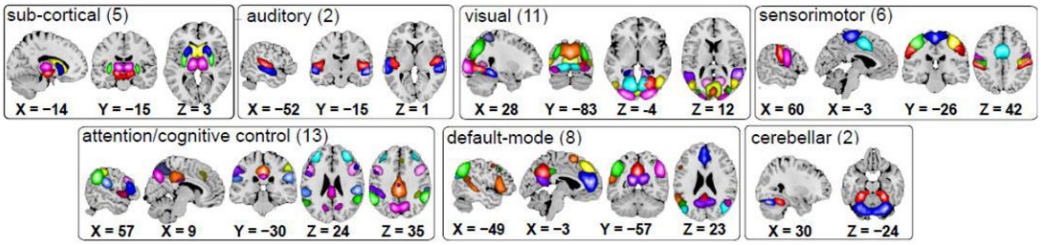

Figure 2.

Spatial maps of selected 47 independent components grouped based on functionality into 7 categories: subcortical (5 components), auditory (2 components), visual (11 components), senorimotor (6 components), attention/cognitive control (13 components), default-mode network (8 components) and cerebellar (2 components).

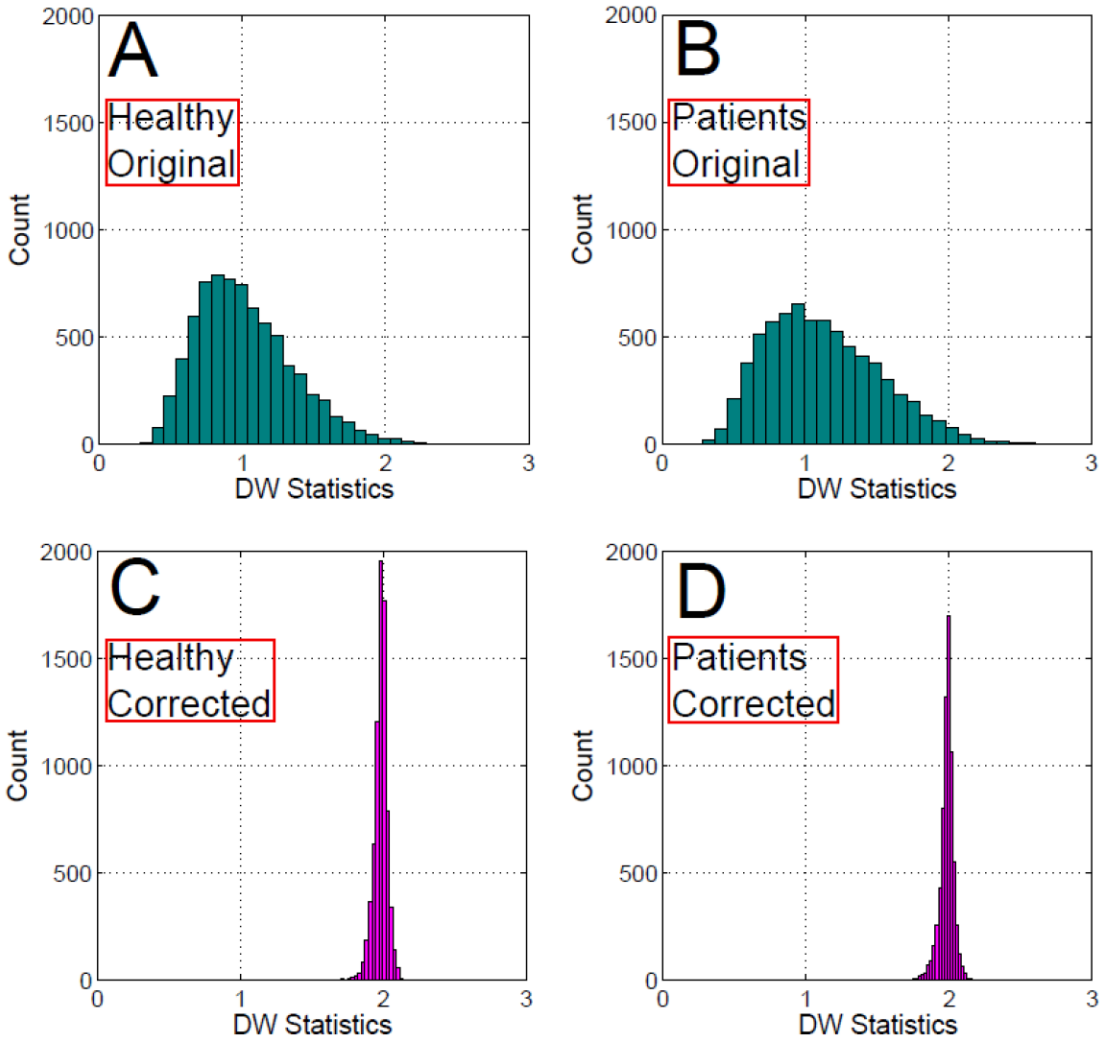

Figure 3.

Durbin-Watson statistics histogram for **A**: Uncorrected IC time-series for healthy controls **B**: Uncorrected IC time-series for schizophrenia patients **C**: Corrected IC time-series for healthy controls **D**: Corrected IC time-series for schizophrenia patients. Autocorrelation correction successfully concentrated DW statistics around 2 which is a sign for absence of autocorrelation.

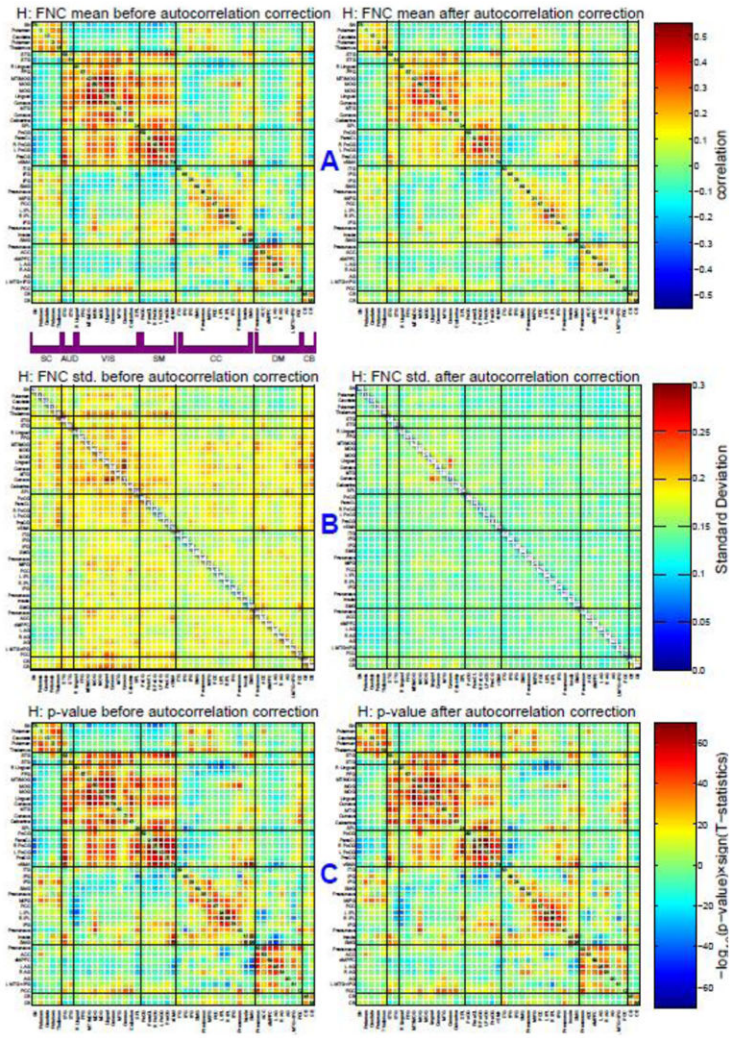

Figure 4.

A,B: Mean and standard deviation of FNC grouped by functionality of brain networks (Figure 2) for healthy controls before and after autocorrelation correction. **C**: -log(p-value) ×sign of t-statics after subject-wise 1-sample t-test on each FNC pair before and after autocorrelation correction. Although the FNC values alter noticeably before and after autocorrelation correction, p-values remain very similar.

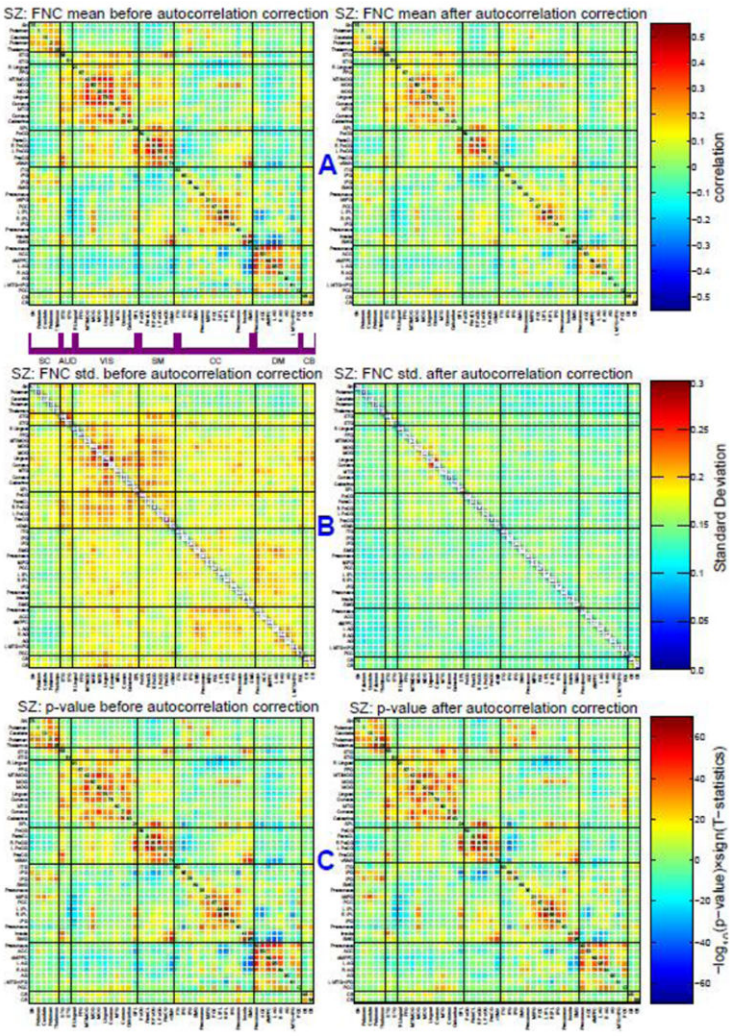

Figure 5.

A,B: Mean and standard deviation of FNC grouped by functionality of brain networks (Figure 2) for schizophrenia patients before and after autocorrelation correction. **C**: -log(p-value)×sign of t-statics after subject-wise 1-sample t-test on each FNC pair before and after autocorrelation correction. Although the FNC values alter noticeably before and after autocorrelation correction, p-values remain very similar.

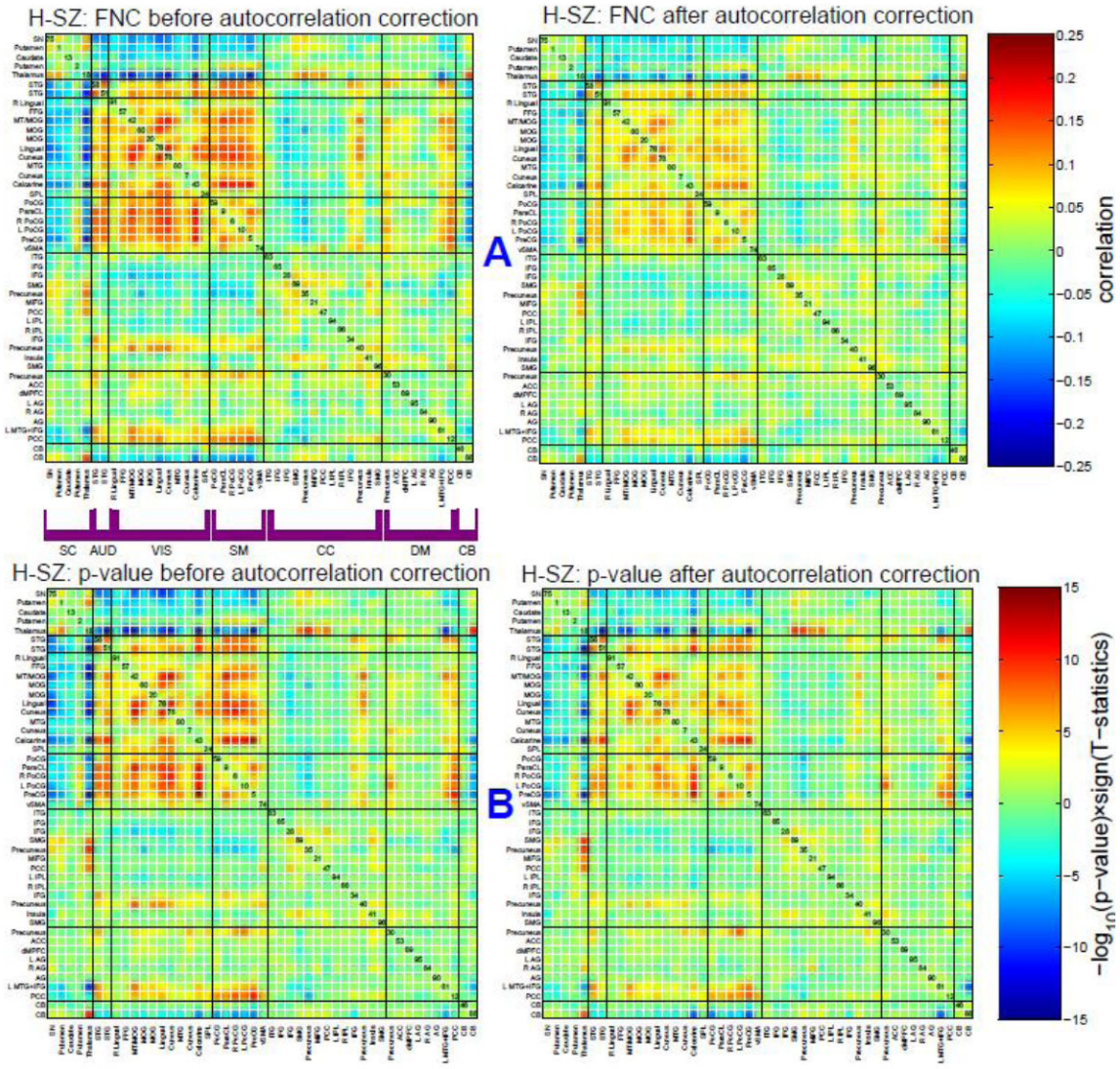

Figure 6.

A: Difference in mean of FNC between healthy controls and schizophrenia patients (healthy-patients) grouped by functionality of brain networks (Figure 1) before and after autocorrelation correction. **B**: -log(p-value)×sign of t-statics after subject-wise 2-sample t-test between controls and patients before and after autocorrelation correction. Although the differences in FNC values between healthy controls and patients alter noticeably before and after autocorrelation correction, p-values of 2-sample t-test remain very similar.

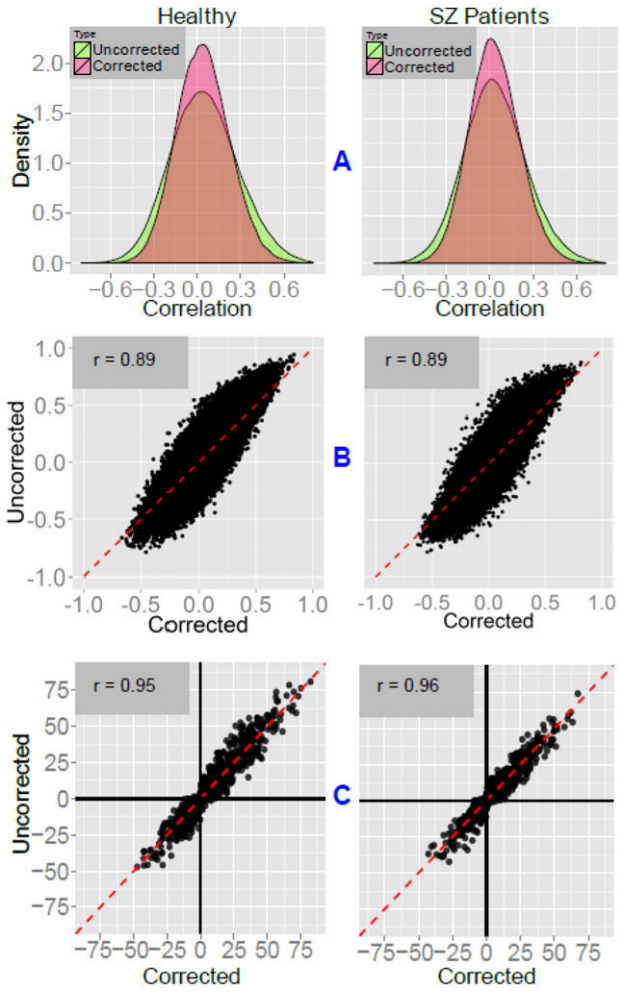

Figure 7.

A: Histogram of corrected and uncorrected FNC values (pooled all subjects and pairs) for healthy controls and schizophrenia patients. **B**: Scatter plot of uncorrected FNC values against corrected FNC values for healthy controls and schizophrenia patients. Correlation coefficient between corrected and uncorrected FNC values is high for both groups (r = +0.89). Compare these results with simulation results in Figure 1B (especially for $\alpha = \beta = 0.5$). **C:** Scatter plot of –log(*p_value*) × *sign* (*T_Statictics*) before and after autocorrelation correction for healthy controls and schizophrenia patients (these are scatter plots of color-coded values in Figure 4C and 5C).

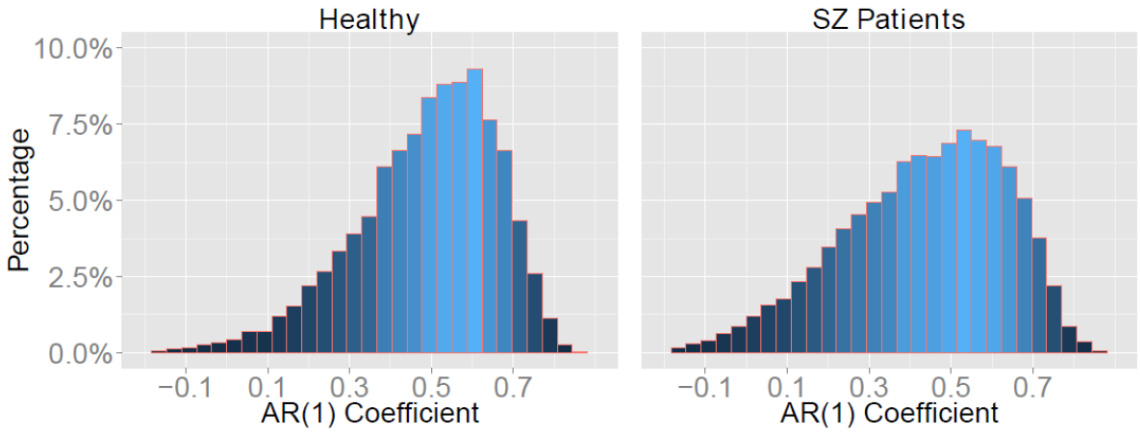

Figure 8.

Histogram of AR coefficient for pooled IC time-series for all subject for healthy controls and schizophrenia patients if all time-series are corrected with AR(1).

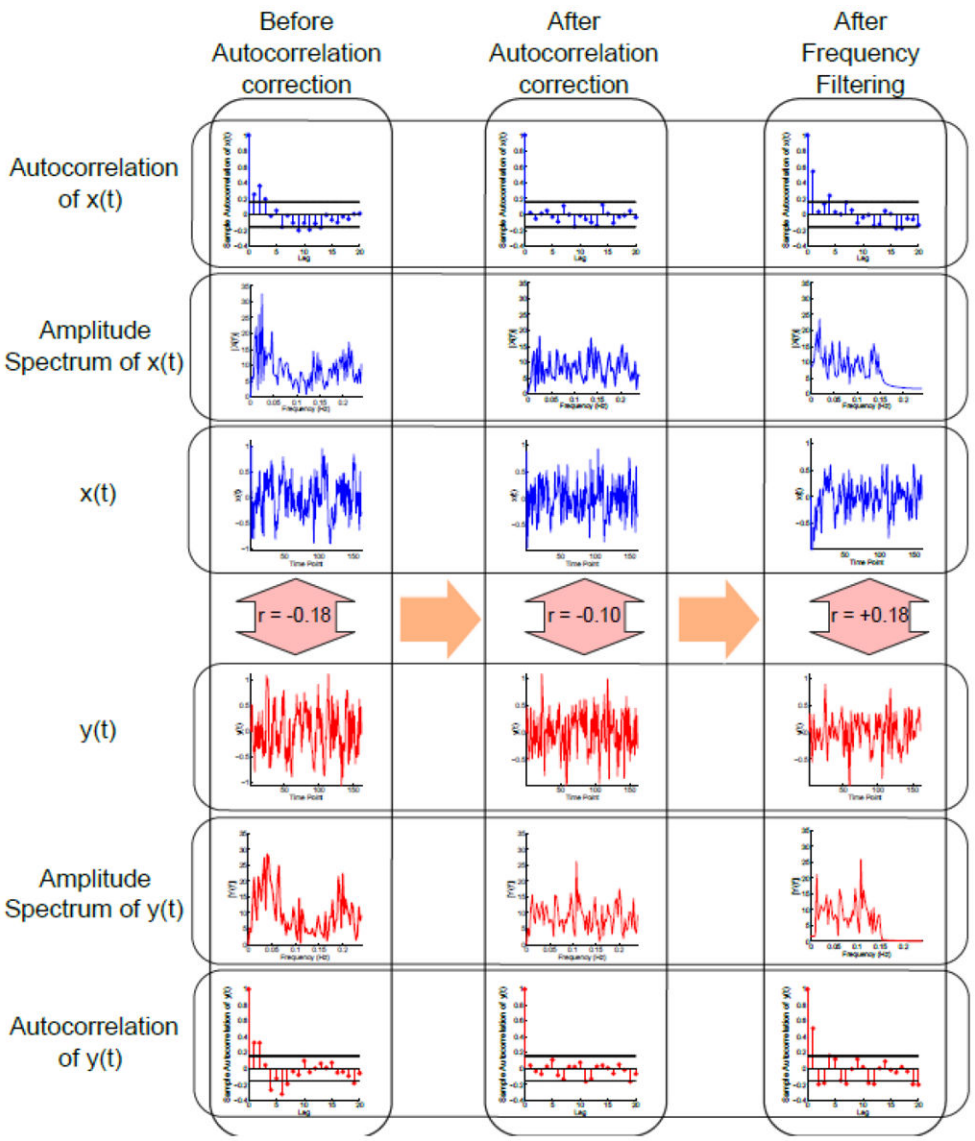

Figure 9.

Autocorrelation function with 95% confidence interval lines and amplitude of frequency spectra for two fMRI time-series, *x*(*t*), y(t) before autocorrelation correction (left column), after autocorrelation correction with AR(4) model (middle column) and after frequency filtering with a order 6 Butterworth passband filter with cutoff frequencies of 0.01 Hz and . 10 Hz (right column). While autocorrelation correction improves the autocorrelation function (all values are inside 95% confidence interval), frequency filtering introduce back the autocorrelation in a more severe and complicated manner.

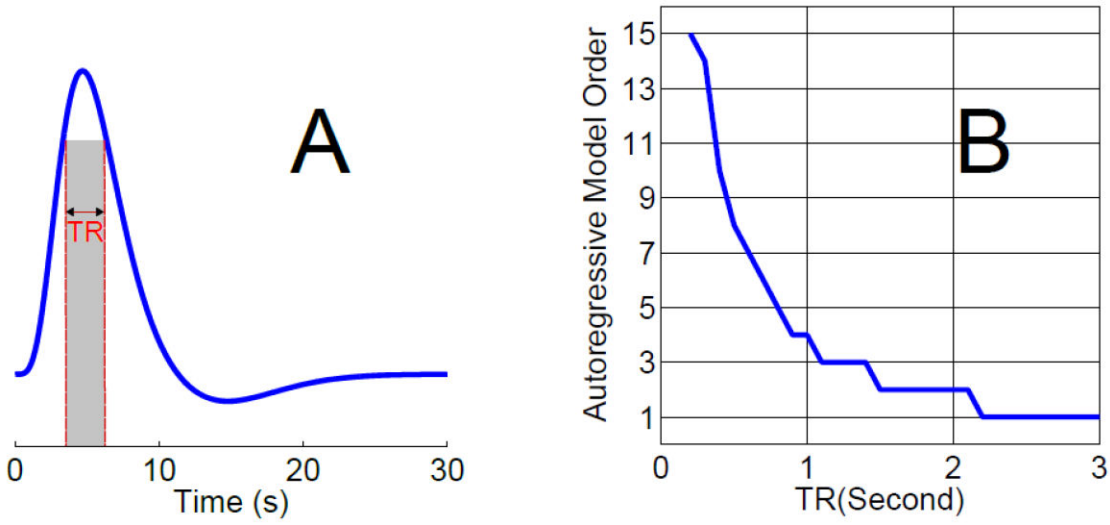

Figure 10.

A: Canonical HRF function **B**: Best model order based on AIC for correcting autocorrelation of samples taken with different *TR* (repetition time) from the HRF function. Best model order increases exponentially as *TR* decreases.

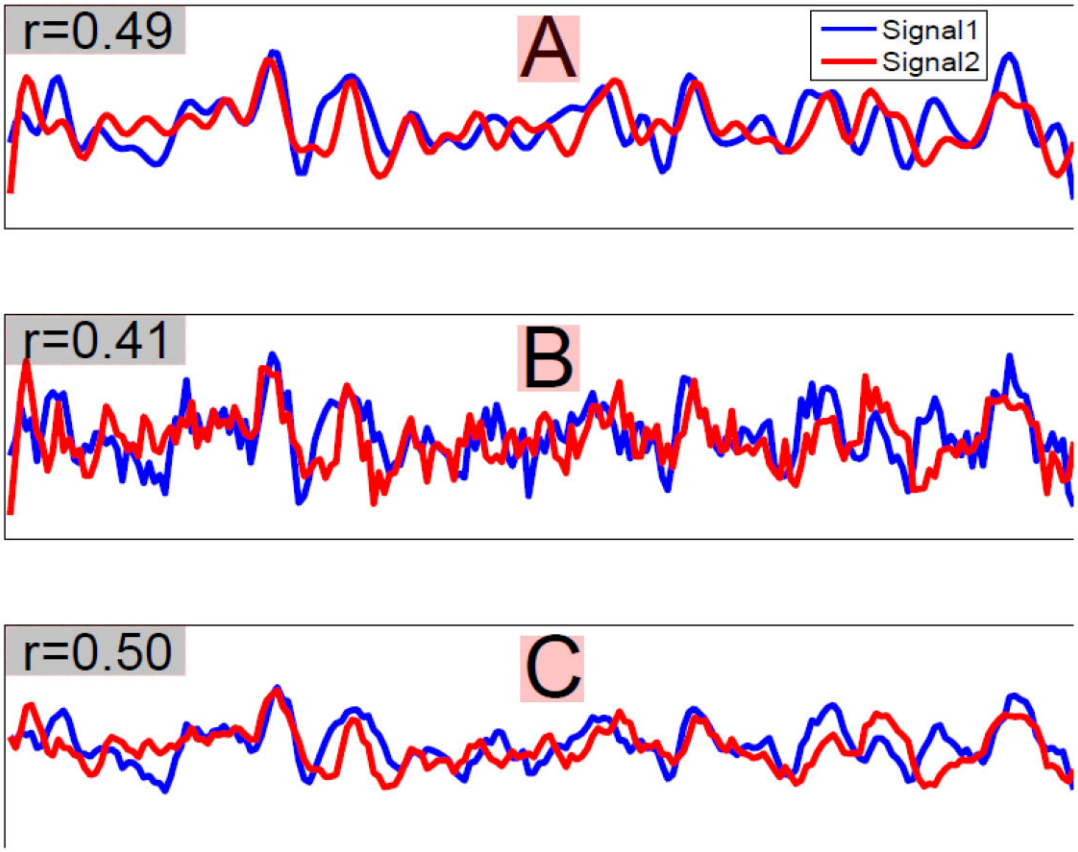

Figure 11.

A: Two correlated low frequency time-series (200 time-points) **B:** After adding high frequency noise to the original time-series in part **A** (*SNR* = 20*db*) **C:** Time-series in part **B** passed through AR(1) process with coefficients of +0.6. Autocorrelation acts as a low pass filter and enhances the correlation between two noisy signals in part **B** close to the original level in part **A**.